

**CONCEPTUALIZATION AND PROCESS SIMULATION OF A CO₂ BASED
METHANOL PRODUCTION PLANT**

Saman Khawaja^{1,2}, Muhammad Rashid Usman^{1,3*}, Rabya Aslam¹

¹Institute of Chemical Engineering and Technology, University of the Punjab, New campus, Lahore 54590, Pakistan

²School of Chemical Engineering, Minhaj University Lahore, Civic Center, Twp, Lahore 54770, Pakistan

³Engineering Research Centre, University of the Punjab, New campus, Lahore 54590, Pakistan

<https://doi.org/10.2298/CICEQ230817003K>

Received 17.8.2023.

Revised 5.2.2024.

Accepted 14.2.2024.

* Corresponding Author: mrusman.icet@pu.edu.pk

Abstract

The present study conceptualizes and simulates a methanol production process through the direct hydrogenation of captured CO₂. CuO/ZnO/ZrO₂ was employed as the catalyst and Aspen HYSYS was used for the process simulation. Configurational optimization of the process flowsheet was carried out using a step-by-step hierarchical approach. Many alternate flowsheets were resulted, and their capital investment, product cost, and profitability measures were calculated. The discrimination among the competing flowsheets was carried out on the basis of net profit and percent return on investment. The retained flowsheet was further analyzed for optimizing the recycle ratio and evaluating the effect of the price of captured CO₂, green H₂, natural gas (fuel), and catalyst on the economic performance of the plant. The optimum value of the recycle ratio was computed to be 4.23. Additionally, it was found that the price of H₂ is the most important parameter in defining the feasibility and profitability of the process. Mathematical correlations were also developed that relate profitability and price of the above-mentioned feed materials.

Keywords: CO₂ capture; CO₂ utilization; Methanol economy; CO₂ Hydrogenation; CuO/ZnO/ZrO₂ catalyst.

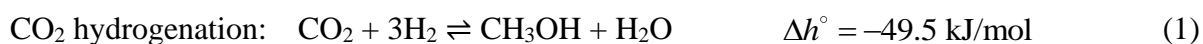
Highlights

- A process plant based on CO₂ hydrogenation to methanol is conceptualized and simulated
- A step-by-step hierarchical procedure is adopted to develop the most profitable flowsheet
- Reactor cooling by boiler feed water with steam generation is found a more favorable solution
- Price of hydrogen has emerged as a major factor in determining the feasibility of the process

INTRODUCTION

Crude oil, natural gas, and coal supply nearly 82% of the world's energy demand [1]. These fossil fuels are a source of a large quantity of human-derived CO₂ that amounted to 34.9 giga tonne, alone in the year 2021 [2]. CO₂ is a greenhouse gas, the second most important after water vapors, that is responsible for increasing the Earth's temperature. Scientists believe that the average temperature rise of the Earth's atmosphere from the preindustrial era must be limited to 2°C [3] to avoid the unparalleled catastrophic effects of global warming. In order to decrease the CO₂ emissions linked with the burning of fossil fuels, the produced CO₂ must be captured and sequestered or utilized in the production of useful chemicals. Utilizing CO₂ in the production of useful chemicals, not only helps in the management of CO₂ emissions, but it also exploits the potential chemical resource of CO₂. One way to utilize CO₂ is to convert it into methanol in the context of so-called "Methanol Economy", an idea initiated by Olah [4]. Methanol is a valuable product that is not only an alternative fuel, but it is also a precursor to many important chemicals. Methanol is a feedstock for gasoline (MTG), olefins (MTO), formaldehyde, tert-amyl methyl ether (TAME), dimethyl ether, acetic acid, methyl tertiary butyl ether (MTBE), methyl esters, etc. When CO₂ for methanol is obtained from an energy source such as biomass or captured from a power plant and hydrogen is produced from the electrolysis of water, realized by a renewable source of energy, the whole process is believed to be green and sustainable.

In the 70s copper-based heterogeneous catalyst, CuO/ZnO/Al₂O₃, was developed [5] for the methanol synthesis realized by the hydrogenation of CO and CO₂. The said hydrogenation process occurs at a modest temperature (200–300°C) [6, 7] and at a fairly high pressure (5–10 MPa) [6, 7] where a high heat of reaction is involved. The direct conversion of CO₂ to methanol occurs under the same operating conditions, but with a lower heat of reaction and the formation of reduced amounts of byproducts [8]. The production of water along with methanol may cause expensive downstream methanol purification and may affect the life of the catalyst [9]. CO₂ to methanol synthesis involves the following three reactions; CO₂ hydrogenation to methanol, reverse water gas shift reaction (RWGS), and CO hydrogenation to methanol:



There are numerous literature studies that discuss the process simulation and economic feasibility of the direct synthesis of methanol from CO₂ and H₂. Van-Dal and Bouallou [10] proposed a flow scheme where they integrated CO₂ to methanol plant with a CO₂ capture facility. The design and simulation of the process were carried out using Aspen Plus. They found that the cost of the capture is considerably reduced as the methanol plant supplies 36% of the thermal energy needed for CO₂ capture. Also, they showed that abatement of 1.2 tonne of CO₂ per tonne of methanol produced is possible. A different source of CO₂ was employed by Matzen et al. [11] as the CO₂ was supplied from an ethanol production facility. Wind-based electrolytic H₂ was used and Aspen Plus software was utilized to develop the methanol synthesis plant. The economic evaluation of the process revealed that the cost of the electrolytic hydrogen is the major factor in defining the feasibility of methanol synthesis. Pérez-Fortes et al. [12] adopted the synthesis scheme of Van-Dal and Bouallou [10] and modified its configuration by applying a pinch analysis. Unlike Van-Dal and Bouallou [10], they developed their flowsheet in CHEMCAD software and performed a rather detailed economic analysis. Comparing their analysis with conventional methanol plants, they estimated a decreased capital cost than the traditional plants, however, the price of raw material, i.e., those of green H₂ and captured CO₂, financially discouraged their proposed scheme. Another study that was targeted to mitigate CO₂ emissions from a bioethanol plant was carried out by Wiesberg et al. [13]. They compared direct CO₂ conversion to methanol (Route A) with CO₂ to methanol by the bi-reforming process (Route B) and used Aspen HYSYS for their work. In bi-reforming, natural gas, steam, and CO₂ were used as reactants to produce syn gas which was converted to methanol. In each case, the methanol synthesis followed a novel scheme where CO₂ was compressed to a restricted pressure in the first reactor and only partially converted to methanol. After separating the methanol, the remaining CO₂ was compressed to a higher pressure and converted in the second reactor. This novel scheme was adopted to save the cost of compression. The authors claimed 5 times more CO₂ consumption in Route A and reasoned that Route A is more profitable than Route B. However, they found neither of the two processes is feasible economically. The flow scheme of Route A was further studied by Borisut and Nuchitprasittichai [14] to minimize the methanol production cost. They applied response surface methodology (RSM) and non-linear programming for the optimization and successfully optimized the process. As a variety of hydrogen sources and production methods can be used for CO₂ hydrogenation, Kiss et al. [15] employed by-product wet H₂ from the chlor-alkaline industry. They applied a stripper column where the wet hydrogen was contacted with the methanol-water mixture obtained in the product separator. They reasoned that this way CO and

CO₂ are virtually removed from the product and wet hydrogen is dried. The process simulation was carried out in Aspen Plus and the results claimed a significant reduction in utilities requirements. Roh et al. [16] reviewed the CO₂ conversion processes and discussed the issues and future possibilities in such processes. They suggested finding new and innovative routes that offer reduced CO₂ impacts, are economically viable, and address improved sustainability aspects. The use of biomass for methanol synthesis was studied by Martín and Grossmann [17]. They described an integrated facility for methanol production from switch grass. The concept was to produce syn gas from the biomass and capture some of the CO₂ present in the syn gas. Both the syn gas and the recovered CO₂ were then used to produce methanol in separate synthesis trains. The authors concluded that massive energy needs and large capital investment are the principal drawbacks of their strategy. The idea of a photocatalytic hydrogen source was employed by AlSayegh et al. [18]. The risk of H₂ and O₂ explosion was prevented by adding captured CO₂ to the system to escape the explosive limits. A membrane separator was then employed to recover a H₂ and CO₂ mixture of 3:1 molar ratio. The flow diagram of Van-Dal and Bouallou [10] was employed and simulated in Aspen Plus. The authors reported a high production cost of methanol in comparison to conventional methanol from natural gas. In an effort to reduce the energy requirements, Szima and Cormos [19] came up with the idea of utilizing the purge stream in a gas turbine and low temperature off-streams in organic rankine cycles. The plant simulation was carried out in CHEMCAD and an economic analysis was carried out. With the above modification, they presented an energy-sufficient plant with decreased operational costs. Realizing the fact that cement production is the biggest source of CO₂ emissions, Meunier et al. [20] routed captured CO₂ from a cement plant to produce methanol. They also performed the life cycle assessment to identify the areas of main environmental concern. Aspen Plus was employed for the simulation and the flow scheme was based on the work of Van-Dal and Bouallou [10]. The process was not found economically practicable owing to the high hydrogen production cost. Also, the environmental analysis found hydrogen supply to be the main environmental concern. In the same year, Nguyen and Zondervan [21] investigated three routes, namely bi-reforming, tri-reforming, and direct hydrogenation of CO₂ to methanol. The analysis was carried out with the help of Aspen Plus. The results demonstrated that reforming processes are more economically practicable though less environmentally friendly and can be employed for an interim period till the CO₂ hydrogenation with H₂ from a renewable source may become economically competitive. An algorithmic approach was used by Lee et al. [22] to optimize the methanol synthesis flowsheet. Similar to the work of Wiesberg et al. [13] and Borisut and Nuchitprasittichai [14], they used

adiabatic reactors in series with interstage condensation of methanol. They successfully solved the superstructure and obtained an economically optimized design. Campos et al. [23] also used a multibed reactor with interstage condensation of methanol. They too found a substantial increase in single pass CO₂ conversion, which helped in reducing the overall cost of the process, especially that associated with the recycle structure. The approach of using interstage methanol separation where enhanced single pass conversion is resulted sounds promising and is expected to significantly improve the plant performance. The simulation of CO₂ hydrogenation to methanol over a non-conventional In-Co catalyst was carried out by Cordero-Lanzac et al. [24]. The authors developed the kinetics over the catalyst and used Aspen Plus for their simulation. Additionally, they carried out the life cycle assessment of the CO₂ hydrogenation plant linked with a cement plant. Their findings suggest that the methanol plant can not completely overcome the emissions of a cement plant. In an effort to reduce the cost of produced methanol, Yousaf et al. [25] combined the solid oxide electrolyzer (SOE) employed for hydrogen generation with a CO₂ hydrogenation plant. A slightly modified flowsheet of Van-Dal and Bouallou [10] was employed and Aspen Plus was used for the simulation. In the modified flowsheet, the waste gases were also sent back to the reactor. The authors found a substantial decrease in the cost of methanol production compared to the literature works with proton exchange membrane (PEM) and alkaline electrolyzers. In a more recent work, Haghighatjoo et al. [26] compared the direct and indirect conversion of CO₂ to methanol. The simulation of the two processes was carried out in Aspen Plus and the operating conditions were optimized. They found that the direct method requires lower fixed capital investment as well as poses decreased environmental threats, whereas the indirect method offers higher net profit. Chiou et al. [27] studied six reactor schemes constituting adiabatic and non-adiabatic reactors and compared the schemes for their economic feasibility. The authors came up with the result that a two-reactor system where a non-adiabatic reactor stage followed by an adiabatic stage is the most economical case. They also developed a suitable control system to handle the changes in flowrates and compositions in their process scheme.

In the literature studies discussed above there are researches that discussed the flowsheet development, however, a systematic approach to developing a conceptual flowsheet is found to be missing. The discrimination of various rival flowsheets based on profitability analysis is also not done in the literature. For example, Lee et al. [22] used an algorithmic approach to reach at their final flowsheet. It is not clear what schemes were compared, but the major focus was on the development of the reactor system (with interstage condensation and separation) and parametric optimization. Borisut and Nuchitprasittichai [14] optimized the parameters for

a selected flowsheet that used adiabatic reactors in series with condensation in between the equilibrium reactors. Roh et al. [16] have only partially studied the CO₂ to methanol process and mostly discussed about the issues of process systems engineering for carbon dioxide conversion processes and their integration with other systems. Martín and Grossmann [17] integrated the methanol synthesis from syn gas produced out of switch grass and the methanol synthesis from CO₂ hydrogenation, where CO₂ was obtained during syn gas purification. Their study focused on the integration of the above two schemes and not flowsheet development for CO₂ hydrogenation to methanol. Chiou et al. [27] selected a single flowsheet and compared different configuration of reactor systems only. They used single adiabatic reactor, single non-adiabatic reactor, two-stage adiabatic reactor. No effort was made towards the development of a process flow scheme.

In the present study, inspired by the original work of Douglas [28], a step-by-step hierarchical procedure is developed to discriminate among the alternate flowsheets and to reach the most profitable flowsheet. Knowledge of process design including heuristics and cost estimation is employed to carry out the technoeconomic analysis of the process with a main focus on the configurational optimization conducted through the methodology developed in the present study. Additionally, CuO-ZnO-ZrO₂, a non-traditional catalyst has been applied for the analysis.

METHODOLOGY

Process and simulation basis

CO₂ captured from a 100 MW natural gas power plant and hydrogen from a green source, i.e., by electrolysis of water using solar or wind energy, were used as the starting point for the simulation. The amount of CO₂ captured was computed for a 60% thermally efficient power plant [29] and for a natural gas of the following composition: 90.45% methane, 3.56% ethane, 3.32% N₂, 0.05% O₂/Ar, 0.8% propane, 0.17% n-butane, 0.16% i-butane, 0.05% n-pentane, 0.07% i-pentane, 0.04% C₆₊, and 1.34% CO₂ [30] with 7 lb_m H₂O/MMSCF gas [31]. 10% excess air was employed, and 40% relative humidity of air was assumed. With 0.4% impurity (N₂) in CO₂ feed [32], 796.7564 kmol/h of CO₂ was calculated that entered at 1 bar and 25°C to the methanol plant. Pure hydrogen gas [33] at 25°C and at a pressure of 30 bar [34] was used in the simulation. Other conditions employed for the simulation are listed below:

- Aspen HYSYS was employed for the steady-state simulation.
- The non-random two-liquid (NRTL) model was applied as the fluid package in association with the vapor phase Soave-Redlich-Kwong (SRK) property model. The NRTL was selected

as polar compounds in the liquid phase were expected to be present and that it has been employed by other researchers [11, 15, 35, 36] as well. For a better estimation of liquid density, the Costald method was selected for the estimation of liquid density [37].

-For CO₂ compression, a three-stage compressor was used where the pressure ratio in each stage was kept same.

-Cooling water inlet was at 90°F (32.22°C) and the outlet was at 120°F (48.89°C). The minimum temperature difference of 10°F (5.56°C) was maintained [28]. The hot stream outlet temperature was therefore kept at 100°F (37.78°C).

-Aspen HYSYS “Conversion Reactor” unit was used to simulate the water-cooled isothermal reactor that operated at 50 bar and 250°C. An isothermal reactor was selected as methanol synthesis from direct CO₂ hydrogenation is moderately exothermic in contrast to methanol from CO (nearly half the heat of reaction for CO₂ hydrogenation compared to that of CO hydrogenation). Therefore, only a moderate rise in temperature in an adiabatic reactor is expected which can be made virtually isothermal in a multitubular reactor. High rates of reaction can be maintained in an isothermal reactor along with an improved yield of methanol compared to an adiabatic reactor. Also, the excess heat evolved from the reaction can be more conveniently utilized for, say, generating steam compared to a multibed reactor with interstage cooling.

-All three reactions outlined above in Eqs. 1–3 were incorporated into the simulation.

-Owing to the superior performance of the CuO-ZnO-ZrO₂ catalyst over CuO-ZnO-Al₂O₃ [38], the former was used in the present study. Arena et al. [38] compared the performance of both these catalysts and found that under identical conditions of 50 bar pressure and 513 K temperature, CuO-ZnO-ZrO₂ gives 22.4% CO₂ conversion and 14.3% methanol yield compared to 19.5% CO₂ conversion and 11.9% methanol yield over the CuO-ZnO-Al₂O₃ catalyst.

Over a particle bed of the zirconia-based catalyst, according to the experimental data of Yang et al. [39] at 50 bar and 250°C, 15% conversion was regarded for the CO₂ hydrogenation reaction (Eq. 1), 10% in the case of the RWGS reaction (Eq. 2), and 50% for the CO hydrogenation to methanol reaction (Eq. 3).

-In each simulation run, the molar ratio of H₂ to CO₂ at the reactor inlet was always kept at a constant value of 3:1. The ratio was fixed by varying the molar flowrate of the inlet (makeup) H₂ flow stream.

-Pumps and centrifugal compressors were considered 75% efficient, while adiabatic compressors were taken as 90% efficient.

-Pressure drop in each heat exchanger was taken as 10 psi (68.95 kPa) which is commonly considered as the maximum allowable pressure drop across a heat exchanger. The pressure drop across the reactor was used as 100 kPa as expected due to the presence of a particle bed.

-Aspen HYSYS “Distillation Column” unit was used for simulating the methanol product column. The column was fitted with a partial condenser, to remove the lighter ends, and it contained 15 theoretical trays. The top pressure was maintained at 110 kPa for which the dew point was remained always higher than 100°F (37.78°C) and cooling water was therefore used in the condenser. Methanol product purity was set at 98.5mol% (99.3wt%) while water purity at the bottom was fixed at 99.9mol%. 99.0mol% of methanol in the distillation column feed was recovered in the distillate product. The number of theoretical trays was optimized in initial trials and in all cases it fulfilled the above requirements.

Flowsheet development

Initially, a trivial flowsheet without recycle, heat integration, and more effective downstream separation was conceived and simulated in Aspen HYSYS. The requisite equipment design was carried out and both the capital and product costs were estimated. Based on these costs, the profitability of the process was computed. Later, a step-by-step hierarchical modification of the flowsheet was realized in light of heuristics and process design understanding. After each change in the flowsheet, the costs and profitability of the process were figured out. A suitable profitability measure was used, that is to be discussed in the next section, to discriminate among the various alternate solutions (flowsheets). By a step-by-step hierarchical approach we mean that for the trivial flowsheet mentioned above, firstly, a recycle structure was introduced and tested to determine whether recycling was important or not. This was followed by product separation where various separation schemes were compared. Knowing the best scheme, the heat integration was carried out and a couple of heat integration strategies were tried. In the last step, the parametric optimization of the final configured flowsheet was carried out. However, only the effect of recycle ratio was studied which was visualized as the most important parameter.

In total, seven flowsheet configurations or cases were constructed as outlined in Table 1. In the initial flowsheet (Case-I), as mentioned earlier, only essential processes and equipment were introduced and no recycle, heat integration, and efficient product separation were employed. While recycle is often necessary for low conversion systems, however, in some cases adding recycle negatively affects the profitability of the plant. For example, with gas recycle, recycle compressor and its associated compression cost have to be considered. Also,

the recycle increases the size of the equipment (heat exchangers, heaters, reactor vessels, coolers, and phase separator vessels) and amount of the utilities required together with the additional piping in the recycle loop, which escalates the associated costs. A recycle and a purge stream were introduced in Case-II. Many recycle ratios were studied and a suitable value of recycle ratio was selected and applied in the subsequent cases. A second, but a low pressure vapor liquid equilibrium (LP VLE) phase separator was used in the next case (Case-III). An absorption column was tried in Case-IV and a stabilizer column was introduced in Case-V. After finalizing the purification step, heat integration was carried out with cooling water and boiler feed water, respectively, in Case-VI and Case-VII. Lastly, the recycle ratio was optimized and the effect of the price of the raw materials, energy, and catalyst on the plant's economics was studied for the optimum case (Case-VII-11).

Table 1

Economic evaluation

For the capital cost estimation, the factorial method based on delivered equipment cost [40] was applied. The purchased cost of equipment was calculated by the cost correlations of Seider et al. [41] as validated by Feng and Rangaiah [42]. A 10% delivery cost was added to the total purchased equipment cost to obtain the delivered equipment cost. 2% and 15% of total capital investment were set as land cost and working capital, respectively. The required information for calculating the purchased cost of equipment was obtained from the simulation results and when needed additional information was obtained through the design methods discussed below:

Heat exchanger: The surface area (A) was calculated from the UA value obtained from Aspen HYSYS and dividing UA by typical overall heat transfer coefficient (U) for the given situation [43]. An average value of the overall heat transfer coefficient is used from the range provided in Sinnott and Towler [43].

Reactor: The weight of the catalyst was calculated from space velocity, conversion, and selectivity data of Yang et al. [39]. Using the calculated weight, the total number of tubes were figured out while considering 1300 kg/m^3 as bulk density of the catalyst. Each tube was 2 in OD and 1.67 in ID with a 25 ft length. The surface area was calculated for the total number of tubes and the cost was calculated for a fixed head heat exchanger.

Vapor-liquid separator: The diameter and length of the vessel were calculated by the method given in Branan [44] and Watkins [45].

Distillation and absorption columns: Diameter of the column was calculated based on the widely used Fair correlation [46]. Operating velocity was taken as 80% of the flooding velocity. Sieve trays were employed, and a 10% downcomer area was used. Overall column efficiency was taken as 60% for a distillation column and 55% for a gas absorber. 18 in tray spacing was used and 5 ft additional height was added to obtain the total column height.

The details about the elements of the capital cost estimation method used in the present study are provided in Table S-1 in the electronic supplement.

For the product cost, again the method of Peters et al. [40] was employed. Labor cost was taken as 15% of total product cost while utilities costs were based on process module costs and calculated from the recommendations of Ulrich and Vasudevan [47]. The non-condensables from the distillation column and purge stream were taken as energy credits and therefore the equivalent cost of energy of these streams was subtracted from the total cost of utilities. The land price was considered paid, so rent on land was taken as zero. 8400 h were taken as working hours in a year. A fixed value of depreciation for each year, taken as 10% of fixed capital investment, was used. The unit price of captured CO₂ was considered to be \$0.0471 [48], \$1.5 for green H₂ [49], \$60/kg for the catalyst (expecting a little higher price than an alumina contained copper based catalyst), and \$7.3/MMBtu (\$6.9188/GJ) for the natural gas [50]. The price of \$1.5 for green H₂ is the best-case wind scenario coupled with a low-cost electrolyzer. The detailed breakdown for the product cost calculation is shown in the electronic supplementary material in Table S2. Additionally, chemical (CO₂) conversion efficiency was also calculated as per Eq. 4.

$$\%CCE = \frac{\text{moles of methanol produced}}{\text{moles of CO}_2 \text{ fed}} \quad (\text{Eq. 4})$$

Net profit (NP), return on investment (ROI), and payback period (PBP, based on fixed capital investment) were calculated for the methanol selling price of \$1.5/kg. Income tax was taken as 35% of the gross profit. For comparison purpose, the selling price of methanol (SPM) for 0% ROI (zero net profit) was also calculated. The formulas employed for the above quantities are given in the electronic supplement in Eqs. S-1 through S-5.

PROCESS DESCRIPTION

Case-I: Fig. 1a shows the flow scheme for Case-I, the simplest among all the flow schemes. CO₂ received from a CO₂-captured plant is compressed from 1 bar to 50.69 bar in a three-stage compressor (K-101) with interstage cooling. H₂ obtained from an electrolyzer at a pressure of 30 bar and 25°C is compressed in a single-stage H₂ compressor (K-102), again, to 50.69 bar.

Both compressors are selected as centrifugal type. The two gases are heated in a fixed head shell-and-tube heat exchanger (HE-102) by high pressure steam. The temperature of the outlet stream (Stream 6) reaches 250°C. The reaction takes place in an isothermal multitubular fixed bed reactor (R-101) at 50 bar and 250°C. As the methanol synthesis process is exothermic, cooling water is used to maintain the isothermal reactor conditions. The product gases are cooled in a floating head shell-and-tube heat exchanger (HE-104) again by cooling water. The cooled product is a vapor-liquid mixture and enters V-101, a vertical high pressure vapor-liquid equilibrium (HP VLE) separator. The gases mainly H₂, CO, and CO₂ vent out at the top while liquid containing primarily methanol and water leaves at the bottom. The pressure of the liquid stream is decreased to 1.5 bar by the help of an expansion valve (VLV-101) and the liquid is directed to a distillation column (T-101) fitted with a partial condenser (fixed head, HE-105) at the top. Non-condensables leave at the top and methanol is recovered as a distillate product. The wastewater is collected at the bottom of the distillation column where low pressure steam is employed in a kettle type reboiler (HE-106).

Case-II: The process flowsheet for Case-II is shown in Fig. 1b. Unlike Case-I, the top product of the HP VLE separator (V-101) is recycled back to the reactor inlet. A recycle compressor (K-103) of centrifugal type is employed for this purpose. As the separator is operated at 48.31 bar, only a small increase in pressure is required for the recycle stream (Stream 9R). Additionally, a small stream (Stream 9P) is also purged to avoid the buildup of the inert present in the feed CO₂.

Fig. 1

Case-III: As shown in Fig. 2a, the liquid leaving the high pressure separator (V-101) is expanded in an expansion valve (VLV-101) to release the gases soluble in the methanol-water mixture. The pressure is decreased from 48.31 bar to 2.19 bar and a second VLE separator (V-102) is operated at this lower pressure. Owing to a large liquid to vapor ratio, the second separator is horizontally oriented. The gases leaving at the top of the separator are also pressurized and recycled back to the reactor. A reciprocating compressor (K-104) is called for this duty. The liquid departing at the bottom of the LP VLE is subjected to further decrease in pressure to reach the distillation column (T-101) inlet pressure of 1.5 bar.

Case-IV: The case is shown in Fig. 2b. The vapors leaving the high and low pressure VLE separators and the vent vapors from the top of the methanol distillation column are pressurized to 51.88 bar, cooled, and sent to the gas absorber (19 sieve plates, T-102). The water leaving the distillation bottom is cooled and used as a solvent in the gas absorber, i.e., a part of the

distillation bottom is cooled to 37.78°C and pressurized to absorber conditions and used as a solvent for methanol recovery. The solvent leaving at the bottom of the distillation column is mixed with the LP VLE separator bottom and sent back to the distillation column. This scheme does not require a separate stripper for solvent recovery.

Case-V: Fig. 2c depicts the flowsheet of Case-V. The LP VLE separator of Case-III is replaced by a stabilizer column (35 sieve plates, T-102) that operates at 5 bar. Better separation of non-condensable gases from methanol-water guarantees the absence of non-condensable gases in the methanol distillation column (T-101). The stabilizer top product (Stream 10R) is also pressurized and recycled.

Fig. 2

Case-VI: Heat integration of Case-III was carried out as shown in Fig. 3a. The reactor outlet gases (Stream 7) are used to preheat the reactants (Stream 5A). An additional heat exchanger (HE-102P) was therefore installed for this purpose. Moreover, the distillation bottom product (Stream 14) was used to heat the feed stream (Stream 11) to the distillation column to reduce the heat load on the distillation column. The product stream was cooled thereafter.

Case-VII: The flowscheme for Case-VII is shown in Fig. 3b. Boiler feed water (Stream bfw) at 200 kPa and 32.2°C was used for cooling in the reactor (R-101) and heated upto the saturated conditions (saturated water at 120.2°C). The saturated water was further heated to saturated steam (Stream s2). Part of the saturated steam was used in the reboiler of the methanol distillation column.

Fig. 3

RESULTS AND DISCUSSION

Flowsheet configuration

The results of simulation and cost analysis for different cases of flowsheets are shown in Table 2. For Case-I, the simplest formulation, the net profit is $\$-6.97 \times 10^7$ (%ROI as -158.0) and the selling price of a kg of methanol for zero net profit is \$4.95. Both a negative net profit and a staggeringly high methanol price are quite undesirable. Upon the addition of a recycle structure (Case-II), however, a huge economic benefit is resulted. For example, for a split ratio (defined as the molar ratio of the flowrate of stream 9P to the flowrate of stream 9R) of 0.02, %ROI is increased from -158.0% to +23.96% and the price of a kg-methanol obtained for zero net profit is reduced from \$4.95 to a much lower value of \$1.37. At this stage, various split ratios (recycle ratios) were tried and a moderate split ratio of 0.02 was selected and fixed to be used in the

analysis of the subsequent cases. The above value of split ratio corresponds to the recycle ratio (RCR) of 3.92 calculated by taking the ratio of the molar flowrate of the recycled stream (9R2) to the molar flowrate of the makeup hydrogen stream (2).

Table 2

As mentioned earlier, in the purification step, the load on the distillation column was decreased by using a LP VLE separator, a gas absorption column, or a stabilizer column, respectively as shown in Fig. 2(a), Fig. 2(b), and Fig. 2(c). Comparing the three cases, the results show that the LP VLE separator is the most economical method of separation in the present situation. Table 2 shows that the %ROI is 24.83, 22.22, and 23.70, respectively, for using the LP VLE separator alone, gas absorber, and stabilizer. Out of the three, the case with gas absorption is not only complicated, but it also provided the highest TCI and the lowest net profit. When compared with Case-II over which Case-III, Case-IV, and Case-V were developed, it is revealed that the addition of either a gas absorber (Case-IV) or a stabilizer (Case-V) is proved an economically poor design with adverse economic benefits. In both cases, TCI increased while the net profit decreased. The use of an LP VLE separator is not only a simplified deal, but it has also incremented about 4% net profit for virtually the same TCI. At this point, the integration of LP VLE separator was approved, and the flowsheet developed hitherto was subjected to heat integration.

For heat integration, as mentioned earlier, two approaches were adopted. In the first scheme, cooling water was used to remove the exothermic heat of reaction from the methanol synthesis reactor. Whereas in the second approach, boiler feed water (bfw) was used that was heated to the saturated liquid state by the excess heat of the reactor. Additionally, a boiler was installed to convert the saturated liquid water to the corresponding saturated steam. As the heat of reaction for CO₂ hydrogenation to methanol is nearly half the heat of reaction for CO hydrogenation, an opportunity was available to use cooling water for cooling the reactor. Boiler feed water owing to the requirements of additional treatment, is much more expensive than simple cooling water. The cost comparison between using cooling water and boiling feed water was therefore considered imperative. Fig. 2 and Fig. 3 show, respectively, the use of cooling water alone in the reactor and the use of bfw in the reactor with steam generation. For both the heat integration cases (Case-VI and Case-VII), a massive improvement is observed over the previous best case, Case-III. Although capital investment has increased, the net profit is also increased and increased quite appreciably. The net profit increased nearly 22% for Case-VI, while it increased about 43% for Case-VII. Comparing Case-VI and Case-VII, a significantly

higher net profit is obtained in Case-VII though at the cost of a little more TCI which resulted in virtually the same %ROI for the two cases. Based on the highest revenue and slightly better %ROI than Case-VI, with lowest methanol price for 0%ROI, Case-VII was received as the best flowsheet configuration.

Effect of recycle ratio

The final flowsheet was additionally analyzed for various recycle ratios. As mentioned earlier, the recycle ratio was varied by varying the split ratio (moles 9P/moles 9R). This was done because it was found much more convenient to set a split ratio in Aspen HYSYS than to fix a recycle ratio. Fig. 4 shows the effect of the split ratio (recycle ratio) on the ROI of the plant. It is clearly revealed that the recycle ratio has a great effect on the economic performance of the plant. Initially, with a decrease in recycle ratio, the ROI is linearly increased, it then reached to the maximum and then decreased steadily. A mathematical equation was developed using TableCurve 2D between the split ratio (SR) and ROI as shown in Eq. 5. An excellent fit of the data with the sum of squares of the errors (SSE) of only 7.01×10^{-6} was obtained. Taking the derivative of the function with respect to SR, the maximum of ROI was obtained at the split ratio of 0.00575.

$$ROI = 0.3266 - 3.1910SR + 2.3189SR^2 - \frac{0.0001046}{SR} \quad (5)$$

where SR is the split ratio defined as moles of the 9P stream divided by moles of the 9R stream.

Fig. 4

Case-VII was rerun using the new split ratio and the sub-case was called Case-VII-11. The material balance for Case-VII-11 is shown in Table 3 whereas Tables S-1 to S-3 in the electronic supplement provide the detailed cost estimation and profitability analysis for Case-VII-11. It can be found from the results that the final flow scheme produced 0.71 kg methanol per kg of CO₂ and that 35 tonne of CO₂ is ready to mitigate every hour.

It is important to mention here that at the steady-state the feed flowrate of nitrogen and the purge flowrate (plus nitrogen leaving any other stream) should be the same. However, Table 3 shows a slight difference in the two flowrates caused by the tolerance selected for the simulation. It was observed that as the split ratio was decreased, the convergence became more and more difficult. A smaller value of tolerance was avoided as it could create more problems in convergence thus giving no result.

Table 3

Effect of the price of feed materials

Case-VII-11 was further studied to observe the effect of the price of CO₂, H₂, fuel (NG), and catalyst (together called feed material) on the economic outcome of the plant. The effect on %ROI and the selling price of methanol (SPM) for 0%ROI is shown in Fig. 5 and Fig. 6, respectively. Fig. S-1 and Fig. S-2 in the electronic supplement, on the other hand, show the effect on NP and PBP, respectively. In each case, as expected, with a decrease in the price of a feed material, profitability is increased, and the payback period and SPM for 0%ROI are decreased. Additionally, it can be noticed that within the ranges of study, the effect is more pronounced for changes in CO₂ and H₂ prices than for changes in the prices of fuel and catalyst. Clearly, the price of H₂ is the biggest factor in defining the profitability of the process. Mathematical relationships were also developed for the graphical curves of Figs. 5, 6, S-1, and S-2 and reported along with the data in the figures.

Fig. 5

Fig. 6

Two generalized correlations that combine the effects of the price of each of CO₂, H₂, NG, and catalyst on %ROI and methanol selling price for 0%ROI were also developed as shown in Eq. 6 and Eq. 7, respectively. For each relationship, 40 data points of Figs. 5, 6, S-1, and S-2 were employed, and SSE was used as the objective function to be minimized. The value of SSE for developing Eq. 6 was 8.78×10^{-5} while it was 3.61×10^{-8} for Eq. 7.

$$\%ROI|_{SPM=\$1.5} = 150.9111 - 417.9215C_{CO_2} - 57.1016C_{H_2} - 1.0137C_{NG} - 0.1510C_{Cat} \quad (6)$$

$$SPM|_{0\%ROI} = 0.3819 + 3.0964C_{CO_2} + 0.4231C_{H_2} + 0.007506C_{NG} + 0.001119C_{Cat} \quad (7)$$

where, C_i is the cost or price of the i th feed material.

Eq. 6 and Eq. 7 can be utilized for calculating %ROI and SPM for 0%ROI for any combination of costs of feed materials discussed above. For example, by halving the H₂ price (\$0.75) which is expected in the near future [51], and keeping all the other costs as such, %ROI is increased

from 29.11 to 71.94 and SPM for 0%ROI decreased from \$1.28 to \$0.97. If in addition, the energy cost is used as \$3.0/MMBtu, %ROI rises to 76.30 and SPM for 0%ROI declines to \$0.93/kg. Furthermore, if the price of CO₂ is reduced to zero as if part of the CO₂ meant for sequestration is routed for methanol synthesis, then %ROI and SPM for 0%ROI, respectively, are calculated as 95.98 and \$0.79/kg.

Comparing the market value of methanol taken as \$0.53/kg [52], the process studied in the present work is found economically unfavorable unless the price of both CO₂ and H₂ is decreased to a very low value. As an example, if the cost of CO₂ is kept at \$0.01/kg and cost of H₂ at \$0.06/kg for energy cost of \$3/MMBtu, the selling price of methanol becomes less than \$0.53/kg. However, inline with the aims of CO₂ mitigation while exploiting the valuable chemical content of CO₂, the proposed process has the potential to be used for further research that may lead it to commercial realization.

CONCLUSION

The process flow scheme for the direct CO₂ hydrogenation to methanol was conceptualized and simulated. The incorporation of a gas recycle greatly benefited the process and a 760% increase in ROI was observed when a recycle stream with a recycle ratio of 3.92 was introduced in the simplified basecase. For improving the separation of light gases, a simple low pressure VLE separator yielded a more cost-effective solution than using a gas absorption system or a stabilizer. The reactor cooling with boiler feed water leading to steam generation was proved to be an economically better approach than cooling with cooling water. The recycle ratio caused a huge impact on the economic performance of the plant. The net profit first increased and then decreased with an increase in the recycle ratio. An optimum recycle ratio was worked out and calculated as 4.30. Comparing the effect of price of CO₂, H₂, NG, and catalyst, the price of green hydrogen has exhibited the biggest effect on the profitability of the process. The study indicates that each year 294 kilotonne CO₂ would be successfully abated and in addition 209 kilotonne methanol would be produced that could be traded to generate a large sum of capital.

Abbreviations

bfw	Boiler feed water
cw	Cooling water
hps	High pressure steam
lps	Low pressure steam
HP	High pressure
ID	Internal diameter
LP	Low pressure
MTG	Methanol to gasoline

MTO	Methanol to olefins
NG	Natural gas
NP	Net profit
NRTL	Non-random two-liquid
OD	Outer diameter
PBP	Payback period
RCR	Recycle ratio
ROI	Return on investment
SPM	Selling price of methanol
SR	Split ratio
SRK	Soave-Redlich-Kwong
SSE	Sum of squares of the errors
TCI	Total capital investment
TPC	Total product cost
VLE	Vapor liquid equilibrium

REFERENCES

- [1] BP, bp Statistical Review of World Energy 2022, seventy first ed., 2022.
<https://www.bp.com/en/global/corporate/energy-economics/statistical-review-of-world-energy.html>
- [2] Z. Liu, Z. Deng, S.J. Davis, C. Giron, P. Ciais, *Nat. Rev. Earth Environ.* 3 (2022) 217–219. <https://doi.org/10.1038/s43017-022-00285-w>.
- [3] Y. Gao, X. Gao, X., Zhang, *Engineering* 3 (2017) 272–278.
<http://dx.doi.org/10.1016/J.ENG.2017.01.022>.
- [4] G.A. Olah, *Angew. Chem. Int.* 44 (2005) 2636–2639.
<https://doi.org/10.1002/anie.200462121>.
- [5] U.J. Etim, Y. Song, Z. Zhong, *Front. Energy Res.* (2020) 545431.
<https://doi.org/10.3389/fenrg.2020.545431>.
- [6] M. Behrens, F. Studt, I. Kasatkin, S. Köhl, M. Hävecker, F. Abil-Pedersen et al., *Science* 336 (2012) 893–897. <https://doi.org/10.1126/science.1219831>.
- [7] K. Stangeland, H. Li, Z. Yu, *Energy, Ecol. Environ* 5 (2020) 272–285.
<https://doi.org/10.1007/s40974-020-00156-4>.
- [8] D.S. Marlin, E. Sarron, Ö. Sigurbjörnsson, *Front. Chem.* 6 (2018) 446.
<https://doi.org/10.3389/fchem.2018.00446>.
- [9] M. Bukhtiyarova, T. Lunkenbein, K. Kähler, R. Schlögl, *Catal. Lett.* 147 (2017) 416–427.
<https://doi.org/10.1007/s10562-016-1960-x>.
- [10] E.S. Van-Dal, C. Bouallou, J. Clean. Prod. 57 (2013) 38–45.
<https://doi.org/10.1016/j.jclepro.2013.06.008>.
- [11] M. Matzen, M. Alhajji, Y. Demirel, *Energy* 93 (2015) 343–353.
<https://doi.org/10.1016/j.energy.2015.09.043>.
- [12] M. Pérez-Fortes, J.C. Schöneberger, A. Boulamanti, E. Tzimas, *Appl. Energy* 161 (2016) 718–732. <https://doi.org/10.2790/89238>.
- [13] I.L. Wiesberg, J.L. de Medeiros, R.M.B. Alves, P.L.A. Coutinho, O.Q.F. Araújo, *Energy Convers. Manage.* 125 (2016) 320–335. <http://doi.org/10.1016/j.enconman.2016.04.041>.
- [14] P. Borisut, A. Nuchitprasittichai, *Front. Energy Res.* 7 (2019) 81.
<https://doi.org/10.3389/fenrg.2019.00081>.
- [15] A.A. Kiss, J.J. Pragt, H.J. Vos, G. Bargeman, M.T. de Groot, *Chem. Eng. J.* 284 (2016) 260–269. <https://doi.org/10.1016/j.cej.2015.08.101>.
- [16] K. Roh, R. Frauzem, R. Gani, J.H. Lee, *Chem. Eng. Res. Des.* 116 (2016) 27–47.
<http://dx.doi.org/10.1016/j.cherd.2016.10.007>.

- [17] M. Martín, I.E. Grossmann, *Comput. Chem. Eng.* 105 (2017) 308–316.
<https://doi.org/10.1016/j.compchemeng.2016.11.030>.
- [18] S. Alsayegh, J.R. Johnson, B. Ohs, M. Wessling, *J. Clean. Prod.* 208 (2018) 1446–1458.
<https://doi.org/10.1016/j.jclepro.2018.10.132>.
- [19] S. Szima, C.C. Cormos, *J. CO₂ Utilization* 24 (2018) 555–563.
<https://doi.org/10.1016/j.jcou.2018.02.007>.
- [20] N. Meunier, R. Chauvy, S. Mouhoubi, D. Thomas, G. De Weireld, *Renewable Energy* 146 (2020) 1192–1203. <https://doi.org/10.1016/j.renene.2019.07.010>.
- [21] T.B.H. Nguyen, E. Zondervan, *J. CO₂ Util.* 34 (2019) 1–11.
<https://doi.org/10.1016/j.jcou.2019.05.033>.
- [22] H.W. Lee, K. Kyeongsu, J. An, J. Na, H. Kim, H. Lee, et al., *Eneregy Res.* 44 (2020) 8781–8798. <https://doi.org/10.1002/er.5573>.
- [23] B.L.de O. Campos, K. John, P. Beeskow, K.H. Herrera Delgado, S. Pitter, N. Dahmen, et al., *Processes* 10 (2022) 1535. <https://doi.org/10.3390/pr10081535>.
- [24] T. Cordero-Lanzac, A. Ramirez, A. Navajas, L. Gevers, S. Brunialti, L.M. Gandía, et al. *J. Energy Chem.* 68 (2022) 255–266. <https://doi.org/10.1016/j.jechem.2021.09.045>.
- [25] M. Yousaf, A. Mahmood, A. Elkamel, M. Rizwan, M. Zaman, *Int. J. Greenhouse Gas Control* 115 (2022) 103615. <https://doi.org/10.1016/j.ijggc.2022.103615>.
- [26] F. Haghighatjoo, M.R. Rahimpour, M. Farsi, *Chem. Eng. Process.* 184 (2023) 109264.
<https://doi.org/10.1016/j.cep.2023.109264>.
- [27] H-H. Chiou, C-J. Lee, B-S. Wen, J-X. Lin, C-L Chen, B-Y Yu, *Fuel* 343 (2023) 127856.
<https://doi.org/10.1016/j.fuel.2023.127856>.
- [28] J.M. Douglas, *Conceptual Design of Chemical Processes*, McGraw-Hill, New York (1988). ISBN-13: 978-0071001953.
- [29] Mitsubishi Power, Gas Turbine Combined Cycle (GTCC) Power Plants.
<https://power.mhi.com/products/gtcc> [accessed 01 August 2023].
- [30] M.A. Sheikh, *Renewable Sustainable Energy Rev.* 13 (2009) 2696–2702.
<http://doi.org/10.1016/j.rser.2009.06.029>.
- [31] W.A. Poe, S. Mokhatab, *Modeling, Control, and Optimization of Natural Gas Processing Plants*, Gulf Professional Pub., New York (2017). <https://doi.org/10.1016/C2014-0-03765-3>.
- [32] S.O. Akpasi, Y.M. Isa, *Atmosphere* 13 (2022) 1958.
<https://doi.org/10.3390/atmos13121958>.
- [33] S.S. Kumar, V. Himabindu, *Mater. Sci. Energy. Technol.* 2 (2019) 442–454.
<https://doi.org/10.1016/j.mset.2019.03.002>.

- [34] S. Lipiäinen, K. Lipiäinen, A. Ahola A., E. Vakkilainen, *Int. J. Hydrogen Energy* (2023). <https://doi.org/10.1016/j.ijhydene.2023.04.283>.
- [35] G. Leonzio, E. Zondervan, P.U. Foscolo, *Int. J. Hydrogen Energy* 44 (2019) 7915–7933. <https://doi.org/10.1016/j.ijhydene.2019.02.056>.
- [36] J. Zhang, Z. Li, Z. Zhang, R. Liu, B. Chu, B. Yan, *ACS Sustainable Chem. Eng.* 8 (2020) 49. <https://doi.org/10.1021/acssuschemeng.0c06336>.
- [37] M.R. Usman, Z. Shahid, M.S. Akram, R. Aslam, *Int. J. Thermophys.* (2020) 41:44. <https://doi.org/10.1007/s10765-020-2622-1>.
- [38] F. Arena, G. Mezzatesta, G. Zafarana, G. Trunfio, F. Frusteri, L. Spadaro, *J. Catal.* 30 (2013) 141–151. <https://doi.org/10.1016/j.jcat.2012.12.019>.
- [39] C. Yang, Z. Ma, N. Zhao, W. Wei, T. Hu, Y. Sun, *Catal. Today* 115 (2006) 222–227. <https://doi.org/10.1016/j.cattod.2006.02.077>.
- [40] M.S. Peters, K.D. Timmerhaus, R.E. West, *Plant Design and Economics for Chemical Engineers*, fifth ed., McGraw-Hill, New York (2003). ISBN-13: 978-0071240444.
- [41] W.D. Seider, D.R. Lewin, J.D. Seader, S. Widagdo, R. Gani, K.M. NG, *Product and Process Design Principles: Synthesis, Analysis, and Evaluation*, fourth ed., John Wiley & Sons, Inc. (2017). ISBN: 978-1119282631.
- [42] Y. Feng, G.P. Rangaiah, *Chem. Eng. August* (2011) 22–29. <https://www.chemengonline.com/evaluating-capital-cost-estimation-programs-2/?printmode=1>.
- [43] R. Sinnott, G. Towler, *Chemical Engineering Design*, sixth ed., Butterworth-Heinemann (2020). ISBN: 978-0081025994.
- [44] C.R. Branan, *Rules of Thumb for Chemical Engineers*, fourth ed., Gulf Professional Pub., New York (2005). <https://doi.org/10.1016/B978-0-7506-7856-8.X5000-2>.
- [45] R.N. Watkins, *Hydrocarbon Process.* 46 (1967) 253–256. <https://dokumen.tips/documents/watkins-r-n-sizing-separators-and-accumulators-hydrocarbon-processing.html?page=1>.
- [46] P.C. Wankat, *Separation Process Engineering: Includes Mass Transfer Analysis*, third ed., Pearson Education, Inc., New York (2012). ISBN: 978-0131382275.
- [47] G.D. Ulrich, P.T. Vasudevan, *Chem. Eng. April* (2006). https://www.chemengonline.com/articles.php?file=2006%2FEng%2FEng04012006_07.html.
- [48] B. Bane, *Cheaper carbon capture is on the way*. PNNL, March 2021. <https://www.pnnl.gov/news-media/cheaper-carbon-capture-way> [accessed 11 August 2023].
- [49] S.R. Bhagwat, M. Olczak, *Green hydrogen bridging the energy transition in Africa and Europe*. European University Institute (2020).

<https://africa-eu-energy-partnership.org/publications/green-hydrogen-bridging-the-energy-transition-in-africa-europe/>.

[50] Markets Energy, <https://www.bloomberg.com/energy> [accessed 16 April 2022].

[51] C. Bettenhausen, Chem. Eng. News 101 (2023). <https://cen.acs.org/materials/electronic-materials/Electrolyzers-tools-turn-hydrogen-green/101/i21> [accessed 20 January 2024].

[52] ChemAnalyst, Methanol Price Trend and Forecast.

<https://www.chemanalyst.com/Pricing-data/methanol-1> [accessed 11 August 2023].

List of Figures

Fig. 1 Simulation flowsheet for: a) Case-I—Basecase; b) Case-II—Introduction of recycle stream with purge.

Fig. 2 Simulation flowsheet for: a) Case-III—Addition of a low pressure VLE separator; b) Case-IV—Addition of a gas absorption unit; c) Case-V—Addition of a stabilizer unit.

Fig. 3 Simulation flowsheet for: a) Case-VI—Heat integration to Case-III with reactor cooled by cooling water; b) Case-VII—Heat integration to Case-III with reactor cooled by boiler feed water leading to steam generation.

Fig. 4 ROI values with a change in split ratio (recycle ratio). Split ratio is moles of stream 9P divided by moles of stream 9R.

Fig. 5 Effect of variation in costs of CO₂, H₂, energy (NG), and catalyst on %ROI. When not varying in the above relationships, the costs were fixed at \$0.0471/kg CO₂, \$1.5/kg H₂, \$7.3/MMBtu energy (NG), and \$60/kg catalyst.

Fig. 6 Effect of variation in costs of CO₂, H₂, energy (NG), and catalyst on the selling price of methanol for 0% ROI. When not varying in the above relationships, the costs were fixed at \$0.0471/kg CO₂, \$1.5/kg H₂, \$7.3/MMBtu energy (NG), and \$60/kg catalyst.

Fig. S1 Effect of variation in costs of CO₂, H₂, energy (NG), and catalyst on the net profit. When not varying in the above relationships, the costs were fixed at \$0.0471/kg CO₂, \$1.5/kg H₂, \$7.3/MMBtu energy (NG), and \$60/kg catalyst.

Fig. S2 Effect of variation in costs of CO₂, H₂, energy (NG), and catalyst on payback period. When not varying in the above relationships, the costs were fixed at \$0.0471/kg CO₂, \$1.5/kg H₂, \$7.3/MMBtu energy (NG), and \$60/kg catalyst.

Table 1 List of cases simulated in the present study

Case	Description	Figure
I	Only the essential equipment is employed and no recycle is used	Fig. 1a
II	Gas recycle stream with a purge is included in Case-I	Fig. 1b
III	A low pressure VLE separator is integrated with Case-II	Fig. 2a
IV	A gas absorber is incorporated in Case-III	Fig. 2b
V	A stabilizer column is employed in Case-II	Fig. 2c
VI	Heat integration is carried out with Case-III, and cooling water is used for reactor cooling	Fig. 3a
VII	Heat integration of Case-III is performed, and boiler feed water is used for reactor cooling with subsequent steam generation	Fig. 3b

Table 2 Results of simulation in terms of cost and profitability measures

Case	TCI (\$)	TPC (\$)	NP* (\$)	ROI* (%)	PBP* (yr)	Methanol price for %ROI = 0 (\$/kg methanol)	CCE, Eq. 4 (%)
I	44120602.04	153890631.15	-69708730.43	-157.996	—	4.9486	14.65
II	70250734.29	270123796.24	16828805.84	23.9553	2.6190	1.3688	93.00
III	70333475.16	271777961.70	17460563.31	24.8254	2.5506	1.3653	93.87
IV	74903672.84	276465625.74	16646098.24	22.2233	2.7666	1.3728	94.90
V	70669945.94	276029877.3	16752064.48	23.7047	2.6394	1.3719	94.82
VI	82651188.15	265819566.18	21306871.09	25.7793	2.4796	1.3353	93.82
VII	96475299.74	260212347.28	24975190.36	25.8877	2.4718	1.3070	93.82
VII-11	100537614.7	268107909.19	29269639.83	29.1131	2.2598	1.2843	97.45

*for price equivalent to \$1.5/kg methanol

Table 3 Material balance results for major streams of Case-VII-11, i.e., Case-VII with split ratio of 0.00575 (RCR of 4.2972)

Stream #	Stream Name	T (°C)	P (bar)	Phase*	Molar flowrate (kmol/h)						
					CO ₂	H ₂	CO	Methanol	H ₂ O	N ₂	Total
1	Feed CO ₂	25.00	1.000	<i>g</i>	793.5694	-	-	-	-	3.1870	796.7564
2	Feed H ₂	25.00	30.00	<i>g</i>	-	2373.0400	-	-	-	-	2373.0400
3	Compressed CO ₂	169.9	51.38	<i>g</i>	793.5694	-	-	-	-	3.1870	796.7564
4	Compressed H ₂	92.91	51.38	<i>g</i>	-	2373.0400	-	-	-	-	2373.0400
5B	Preheater Inlet	62.66	51.38	<i>g</i>	3115.3699	9343.7753	307.9612	56.2431	11.3332	532.4433	13367.1261
5	Heater Inlet	150.0	50.69	<i>g</i>	3115.3699	9343.7753	307.9612	56.2431	11.3332	532.4433	13367.1261
6	Reactor Inlet	250.0	50.00	<i>g</i>	3115.3699	9343.7753	307.9612	56.2431	11.3332	532.4433	13367.1261
7	Reactor Outlet	250.0	49.00	<i>g</i>	2336.5274	7010.8237	309.7491	833.2977	790.1757	532.4433	11813.0169
7A	Product Cooler Inlet	159.3	48.31	<i>g</i>	2336.5274	7010.8237	309.7491	833.2977	790.1757	532.4433	11813.0169
8	HP Separator Inlet	37.78	47.62	<i>g/l</i>	2336.5274	7010.8237	309.7491	833.2977	790.1757	532.4433	11813.0169
9	HP Separator Vapor Outlet	37.78	47.62	<i>g</i>	2328.4598	7007.7248	309.5453	55.5922	11.1873	532.4263	10244.9357
9P	Purge	37.78	47.62	<i>g</i>	13.3886	40.2944	1.7799	0.3197	0.06433	3.0615	58.9084
9R	HP Separator Recycle	37.78	47.62	<i>g</i>	2315.0711	6967.4304	307.7654	55.2725	11.1229	529.3649	10186.0273
9R2	Recycle	46.81	51.38	<i>g</i>	2321.8005	6970.7353	307.9612	56.2431	11.3332	529.2563	10197.3297
10	HP Separator Liquid Outlet	37.78	47.62	<i>l</i>	8.0676	3.0989	0.2038	777.7055	778.9884	0.01701	1568.0813
10A	LP Separator Inlet	37.37	2.189	<i>g/l</i>	8.0676	3.0989	0.2038	777.7055	778.9884	0.01701	1568.0813
10B	LP Separator Liquid Outlet	37.37	2.189	<i>l</i>	1.2592	0.006298	0.05885	776.7348	778.7781	-	1556.8372
10R	LP Separator Gas Recycle	37.37	2.189	<i>g</i>	6.8085	3.0400	0.1975	0.9707	0.2104	0.01699	11.2441
11	Distillation Column Feed	63.53	1.500	<i>g/l</i>	1.2592	0.006298	0.05885	776.7348	778.7781	-	1556.8372
12	Vent	62.59	1.100	<i>g</i>	1.1780	0.05772	0.006060	6.9995	0.04676	-	8.2880
13	Methanol Product	62.59	1.100	<i>l</i>	0.08120	0.001132	0.0002374	768.9674	11.6276	-	780.6776
14	Distillation Bottoms	111.2	1.500	<i>l</i>	-	-	-	0.7679	767.1038	-	767.8716
14B	Wastewater	42.71	1.810	<i>l</i>	-	-	-	0.7679	767.1038	-	767.8716

* *l*: liquid; *g*: gas

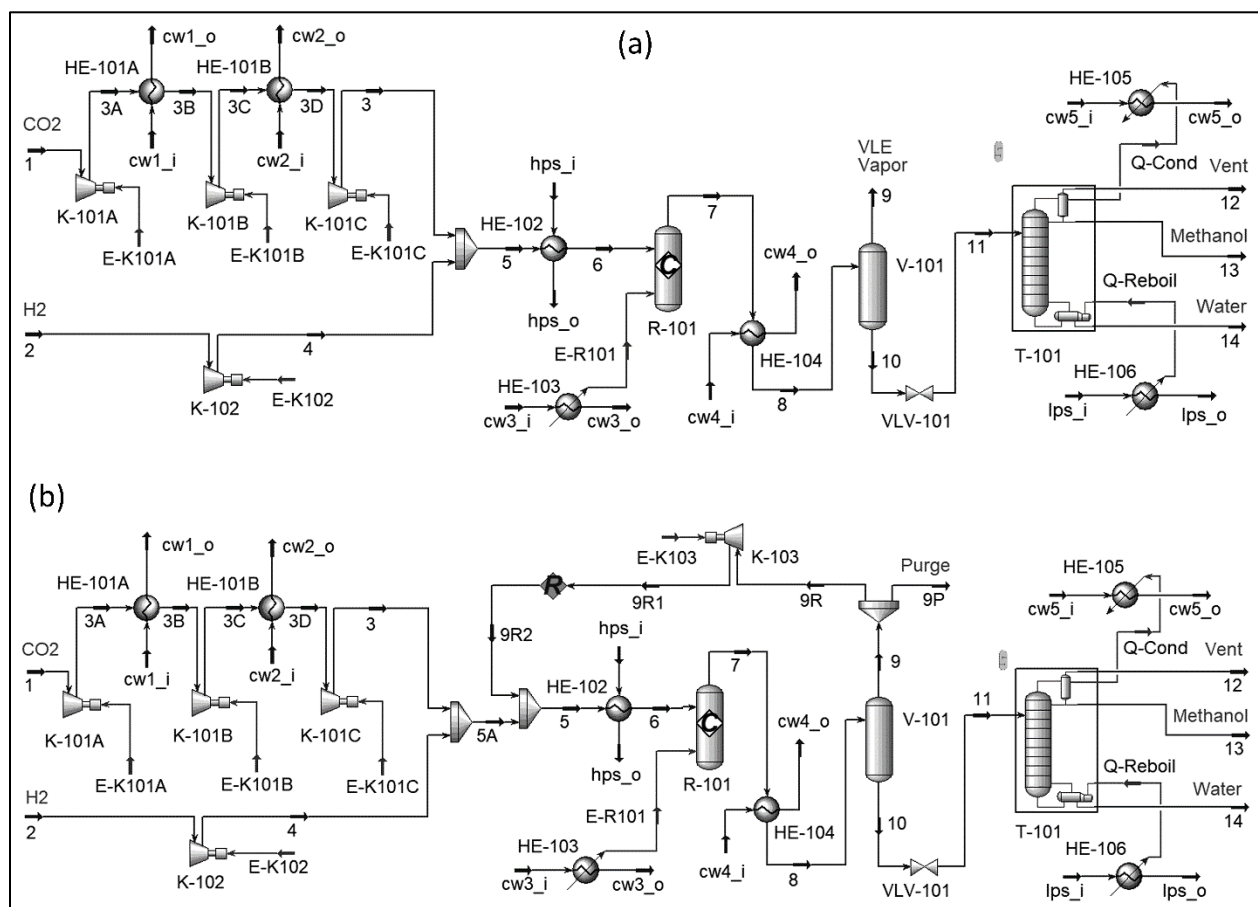


Fig. 1

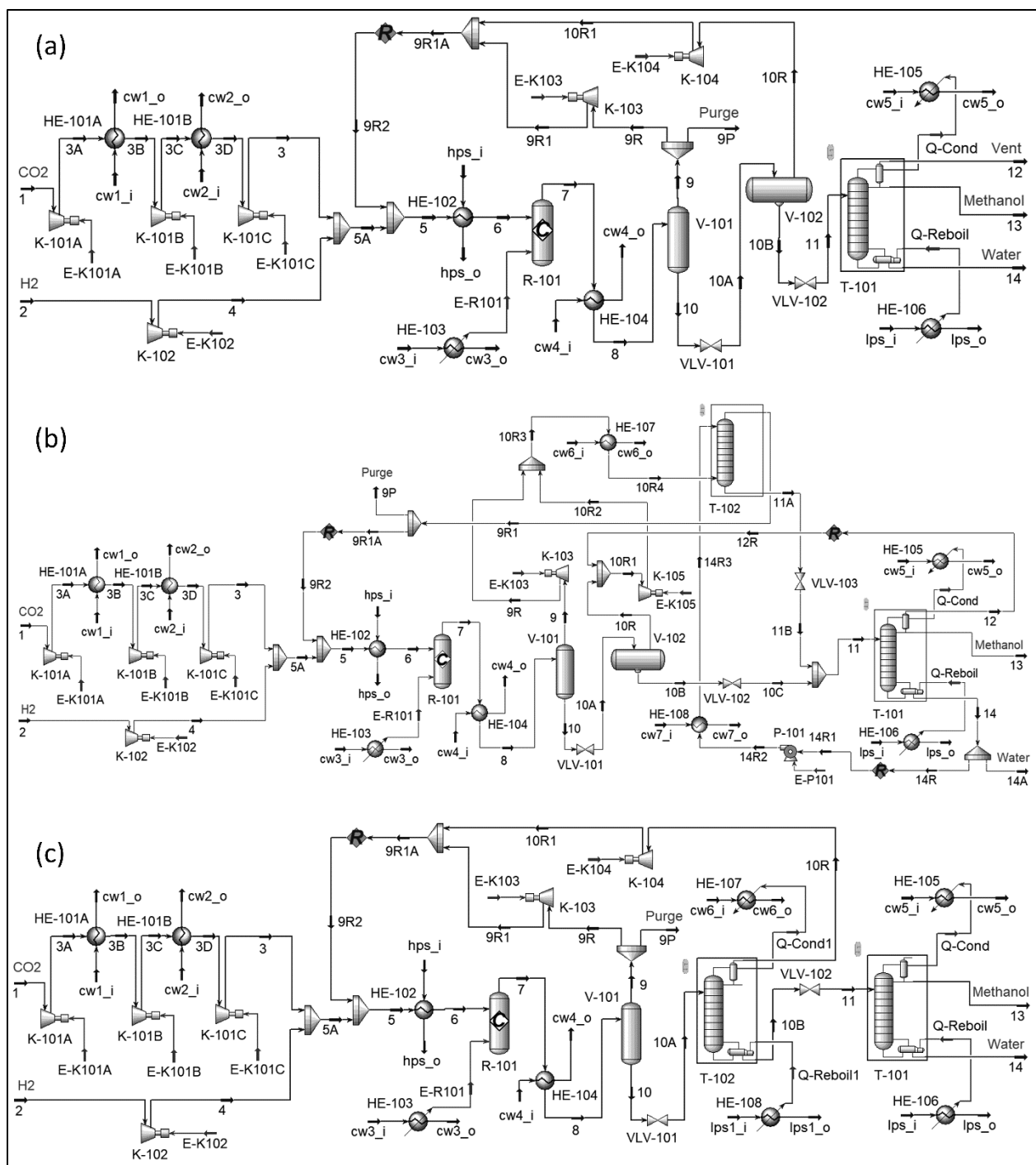


Fig. 2

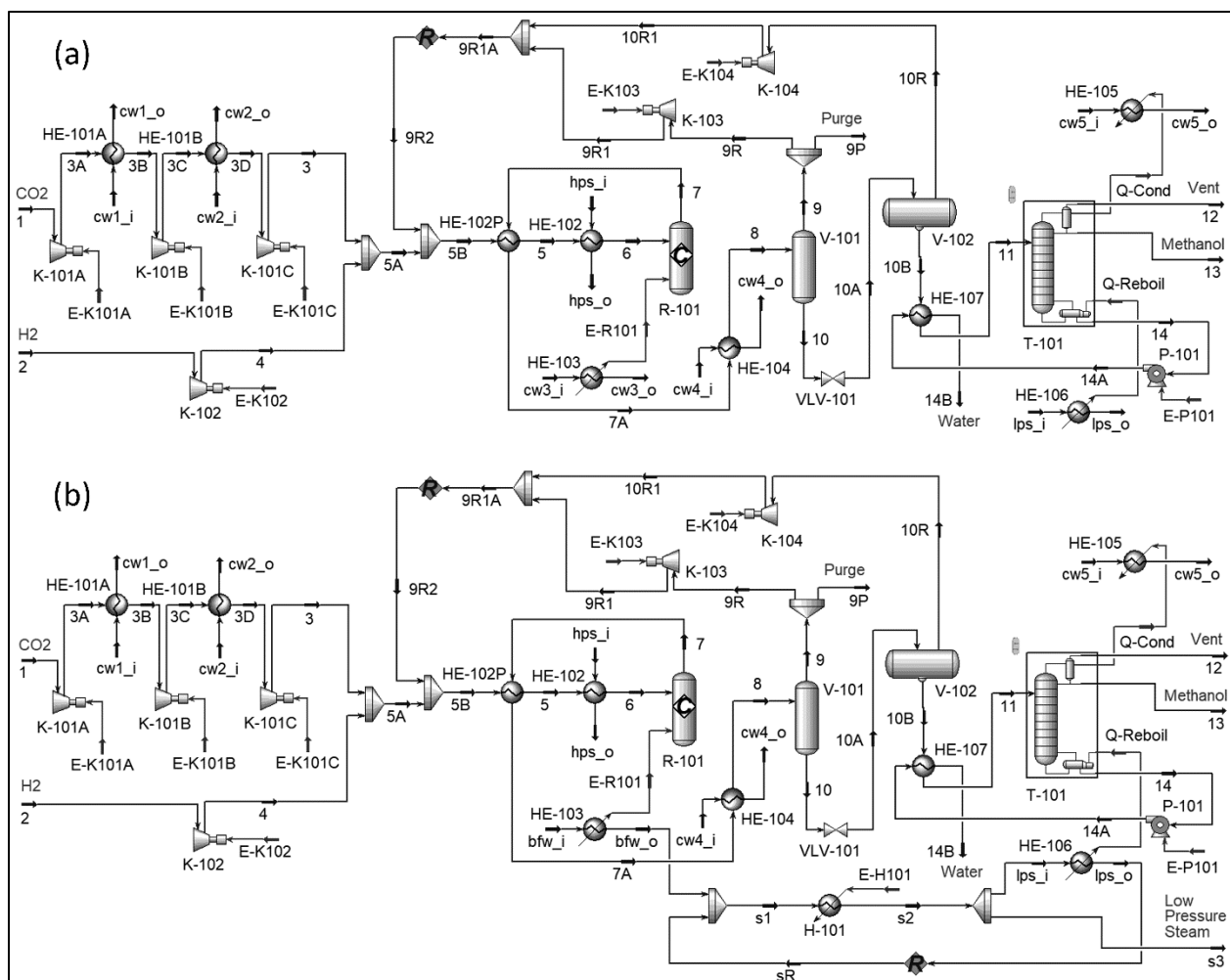


Fig. 3

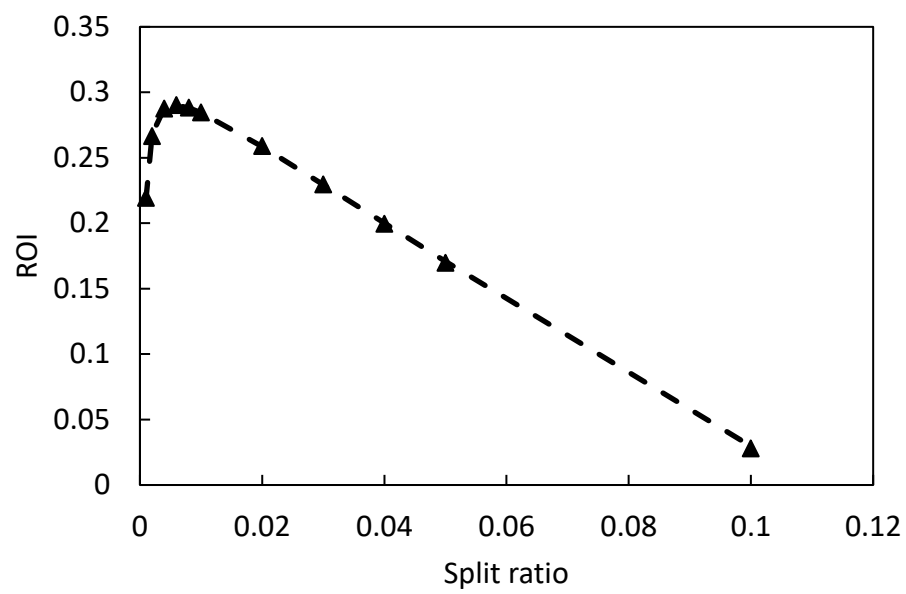


Fig. 4

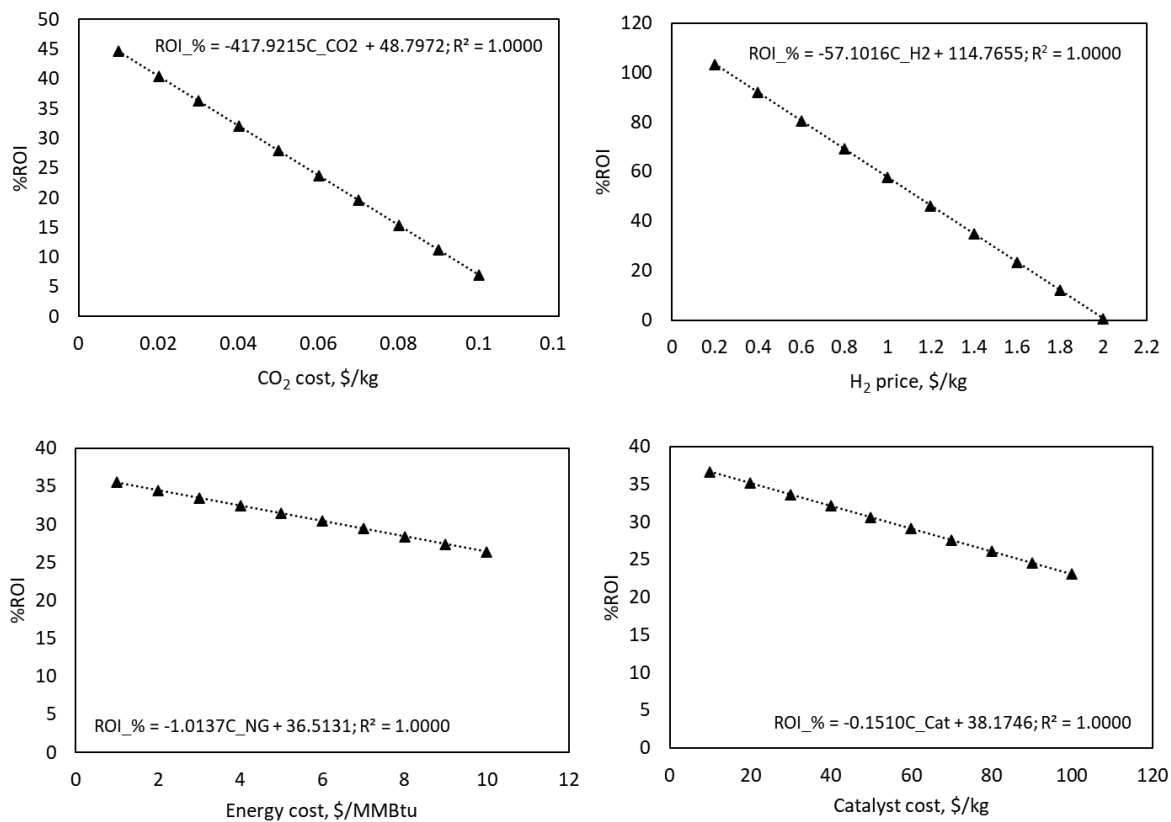


Fig. 5

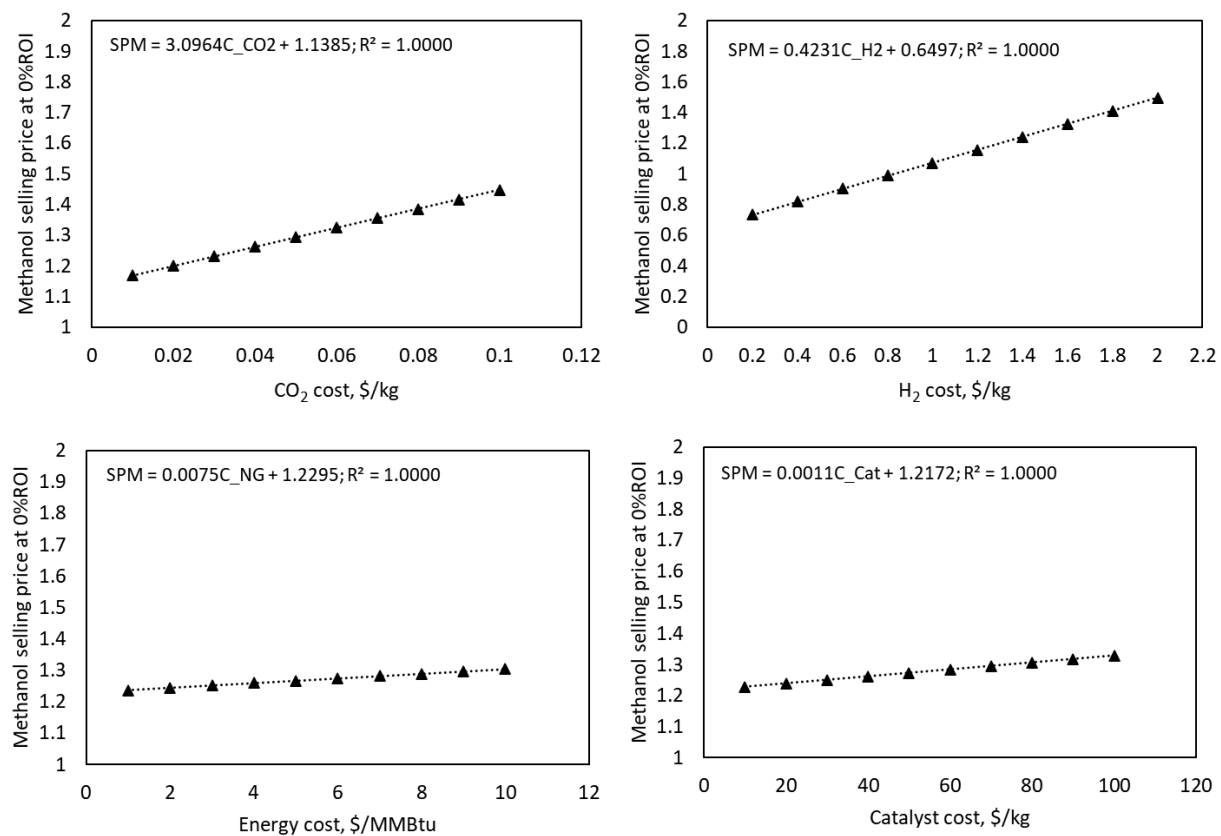


Fig. 6